Top Catal (2011) 54:101–107
DOI 10.1007/s11244-011-9647-4

ORIGINAL PAPER

Kinetic Monte Carlo Simulation of Molecular Processes on Supported Metal Particles

J. L. Sales · M. V. Gargiulo · G. Zgrablich

Published online: 21 January 2011

Abstract A general model is proposed to describe the kinetics of molecular reactions taking place on supported metal particles, which are deformed by the effect of temperature, through kinetic Monte Carlo simulations. The model is applied to the study of the CO oxidation reaction. The effects of adsorbate–adsorbate and adsorbate–metal interactions and of CO and metal atoms diffusion on the reaction window and the overall reaction rate are determined.

Keywords Catalytic reactions · Supported metal particles · Monte Carlo simulation

1 Introduction

Important advances have been achieved in the last few decades in the knowledge about surface chemistry and catalytic reactions on metals in ideal conditions, i.e. in ultra-high-vacuum and on single-crystal surfaces [1]. However, different factors are responsible for the fact that this knowledge cannot be extrapolated directly to overcome the gap between ideal and real systems, among them we have that the active phase consists of supported metal nanoparticles, which expose different crystal facets and may undergo shape deformations during the reaction process, and that the reaction takes place usually at high pressure [2]. The advancement in surface science experimental techniques and the modelling of processes through kinetic Monte Carlo simulations have made possible the study of some of these factors, especially the effects due to the finiteness and shape of supported metal particles [3–8]. Among these studies particular attention has been devoted to stochastic simulations of the monomer–dimer reaction on supported metallic nanoparticles, taking into account the deformation and roughening of the metallic particle due to temperature and energetic effects [7, 8]. In the present work we extend these studies in order to determine the effects of adsorbate–adsorbate and adsorbate–metal interactions on the kinetics of the monomer–dimer reaction, in particular the CO oxidation reaction. Interactions among adsorbed species have proven to play a relevant role in the characteristics of the kinetics of catalytic reactions in many ideal systems [9–11], and it is reasonable to believe that they will also affect the kinetics on supported nanoparticles. In our study we intend to determine how the kinetics of $CO + O_2$ reaction on supported metallic nanoparticles, presenting initially a cubic shape with a (100) facet, is affected by temperature and metal atoms diffusion roughening, CO diffusion both on the metal particles and the support (spillover) and adsorbate–adsorbate and adsorbate–metal interactions, in relation to the predictions of the pioneering ZGB model [12] proposed for an ideal system in 1986.

In Sect. 2 we describe the model to be used and the simulation method, results will be presented and discussed in Sect. 3 and, finally, general conclusions will be given in Sect. 4.

2 Model and Simulation Method

We use a lattice-gas model similar to that proposed in Refs. [7, 8]. The supported nanometric metal particle is

J. L. Sales · M. V. Gargiulo
IEE, Universidad Nacional de San Juan, Av. Ej. De los Andes 950, 5700 San Luis, Argentina

J. L. Sales · M. V. Gargiulo · G. Zgrablich (✉)
INFAP, CONICET-Universidad Nacional de San Luis, Av. Ej. De los Andes 950, 5700 San Luis, Argentina
e-mail: giorgio@unsl.edu.ar

represented initially by a simple cubic $N_X \times N_Y \times N_Z$ lattice whose basis is located at the center of an $M_X \times M_Y$ square lattice representing the sites of the supporting surface. Nearest-neighbor (NN) attractive interactions are assumed to exist between metal atoms (J_{MM}) and between a metal atom and a site of the support (J_{MS}). The system (particle + support) is immersed in a gas phase composed by a mixture of CO and O_2 with partial molar fractions Y_{CO} and Y_{CO_2} such that $Y_{CO} + Y_{O_2} = 1$. The following processes are going to be considered:

(a) *Thermal deformation of the metal particle*

At any time the shape of the metal particle is given by a distribution of columns of atoms of different heights. The surface of the metal particle which will be useful for adsorption of species from the gas phase is given by the upper atoms of each column. This surface will present terraces of different number of metal atoms. A metal atom M may perform a diffusive jump from a site on top of a metal atoms column to a NN site on top of another metal column or to a NN site on the support. The transition probability for a diffusing step is given by the Metropolis rule

$$p_{i,f} = \min\{1,\ \exp[-(E_f - E_i)/k_B T]\} \quad (1)$$

where E_i and E_f are the initial and final configurations energies, respectively, k_B is the Boltzmann constant and T the temperature.

This process with no further restrictions, however, would lead to the complete dispersion of the metal particle over the support at any temperature. This does not occur in practice due to long range cohesion forces and to surface free energy effects, which are not included in the NN interactions considered above. To take into account these effects we impose the further restriction that a diffusion jump can be finally accepted only if the final dispersion of the distances, d, of the metal atoms from the center of the basis of the particle, defined by

$$\sigma = \left(\langle d^2 \rangle - \langle d \rangle^2\right)^{\frac{1}{2}} \quad (2)$$

is smaller or equal than the initial dispersion.

Through this diffusive process the metal particle shape, starting from an initially perfect cubic structure of $N_X \times N_Y \times N_Z$ sites, will evolve toward a more disordered shape consisting of a collection of columns of metal atoms of different heights spreading a greater area on the support than the initial $N_X \times N_Y$ sites, finally reaching a characteristic fluctuating steady state shape which will depend on the temperature and the interaction parameters. In our simulations the achievement of the steady state was monitored through the relative change in the dispersion σ of the particle.

(b) *Catalytic reaction*

During the reaction process the following elementary steps will be considered:

CO adsorption: $CO(gas) + s \rightarrow CO(ads)$

O_2 dissociative adsorption: $O_2(gas) + 2s \rightarrow 2O(ads)$

CO oxidation reaction: $CO(ads) + O(ads) \rightarrow CO_2(gas) + 2s$

CO and M diffusion

It should be stressed that CO adsorption can take place both on metal and support sites, while O_2 dissociative adsorption and the oxidation reaction can only take place on two NN metal atoms on top of columns of the same height, and that transition probabilities for all elementary steps, except O_2 dissociative adsorption and diffusion steps (as explained below), are taken to be 1.

The simulation procedure follows the classical ZGB method [12] with the addition of diffusion processes for CO and metal atoms M. The diffusion of all species will be in general affected by NN lateral interactions W_{AB} among the different species present in the system, so that A and B stand for CO, O and M. A diffusion step will occur with probability $p_{i,j}$ given by Eq. 1, where now E_i and E_j must include all NN lateral interactions W_{AB}. The diffusion of metal atoms, of course, will be subject to the additional restriction described in (a). The O_2 dissociative adsorption step, once 2 NN vacant metal sites are available, will also be executed with a transition probability given by Eq. 1, where NN lateral interaction energies of each O atom with other adsorbed species and with metal atoms will be taken into account. This is necessary due to the fact that oxygen surface diffusion is practically zero and any changes in the distribution of surface O atoms due to interactions must arise during the adsorption process. As it is usual at the temperatures to be used in this study, we neglect O_2 molecular adsorption.

The simulation starts from a "nude" metal particle initially prepared at a temperature T by the procedure described in (a). A molecule, CO or O_2 is chosen from the gas phase with a probability given by its molar fraction and an adsorption step is attempted according to the conditions given above. If the adsorption step is successful, then the neighborhood is explored in order to execute a reaction step. For each adsorption attempt, 10 diffusion attempts are executed. The approach to the steady state is monitored through the change in surface coverage for each species.

3 Results

In our simulations the following lattice dimensions have been used: $N_X = N_Y = 21, N_Z = 10$ (this is equivalent to a

metal particle 8 nm wide and 4 nm high), $M_X = M_Y = 200$. Equilibration in the particle shape was considered attained when fluctuations in the particle dispersion were $\Delta\sigma < 10^{-4}$. During the reaction process, the steady state was considered attained when fluctuations in the coverage of any adsorbed species changed by less than 10^{-3} over the last 10^3 Monte Carlo Steps (MCS). One MCS corresponds to $M_X \times M_Y$ adsorption attempts. All results were averaged over 100 samples of the deformed metal particle for each temperature. In all figures the subscripts A, B and AB, have been used in representation of CO, O and CO_2, respectively.

Figure 1 shows the effect of temperature on the deformation of a metal particle with interaction energies: $J_{MM} = -10$ kJ/mol, $J_{MS} = -2.5$ kJ/mol. In (a) we can see the original non-deformed particle, while (b), (c) and (d) correspond to 500 K, 700 K and 900 K, respectively. It can be seen how the dispersion of the distribution of metal column heights increases with temperature, producing a rougher particle, while the spatial dispersion of metal atoms in the particle, with respect to the center of the particle basis remains approximately constant. At higher temperature (1100 K, not shown here) the dispersion of

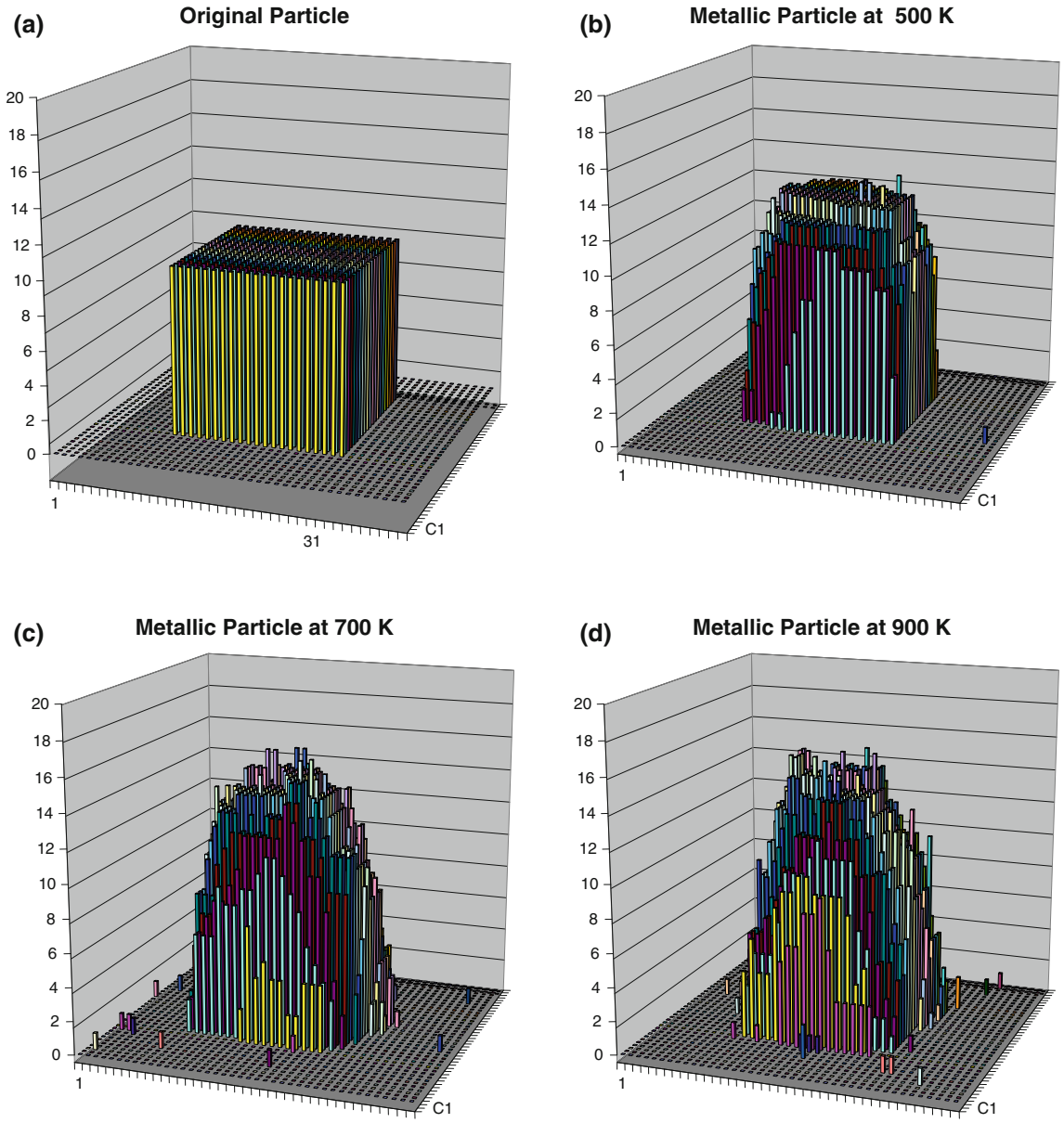

Fig. 1 Simulation snapshots of the metal particle deformation by temperature effect: **a** original undeformed particle and **b–d** equilibrium shape at 500, 700 and 900 K. Interaction parameters: $J_{MM} = -10$ kJ/mol, $J_{MS} = -2.5$ kJ/mol

metal atoms on the support becomes important and, in general it is larger for lower values of the ratio J_{MM}/J_{MS}.

In order to study the reaction process on the supported nanoparticles deformed by thermal effects, we begin with the original undeformed particle, which will be taken as the reference system. Figure 2 shows our reproduction of the classical ZGB results for non-interacting particles without CO diffusion (a) and the modifications due to CO diffusion (b). In each figure, the upper graph represents the steady state coverage for each species as a function of Y_{CO}, while the lower graph represents the reaction rate in the steady state regime, R_{CO_2}, obtained as the ratio between the number of desorbed CO_2 molecules and the number of adsorption attempts. The well known behavior of the reaction window is correctly reproduced in these results: the upper limit of the reaction window remain unaffected by CO diffusion, while the lower limit is extended toward much lower concentrations of CO in the gas phase, and the reactivity is increased, due to the fact that poisoning of the surface with O is strongly depressed by the mobility of CO. It is important to recall that in the ZGB model, at low Y_{CO} values, adsorbed O atoms form compact large islands and the reaction takes place on the periphery. In the ZGB model these large O islands are simply due to the fact that molecular oxygen dissociates on two NN metal atoms. The existence of oxygen islands has been observed in STM studies [13], however the observed islands are not quite compact, with the presence of many irregularly shaped vacant regions.

Figure 3 stresses the effect of the particle deformation by temperature, again for non-interacting particles, corresponding to $T = 500$ K. When no diffusion is taken into account (a), the reaction window is similar to that corresponding to the case of the original particle but, unlike that case, the poisoning of the surface at low CO concentration in the gas phase is not a consequence of saturation of the

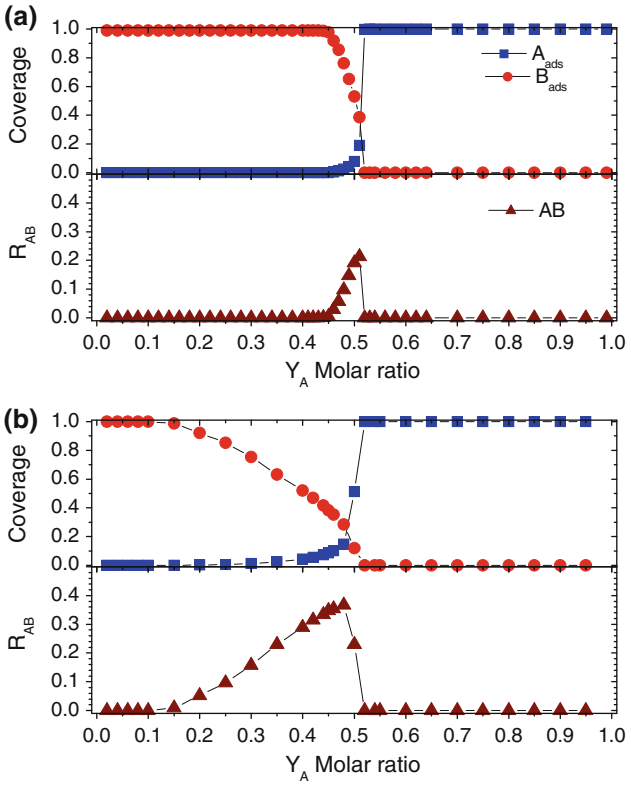

Fig. 2 Classical behavior of the surface coverage (*upper* graph) and reaction rate (*lower* graph) as a function of CO molar fraction in the gas phase, for an undeformed metal particle with the assumptions of the ZGB model: **a** without CO diffusion and **b** with CO diffusion

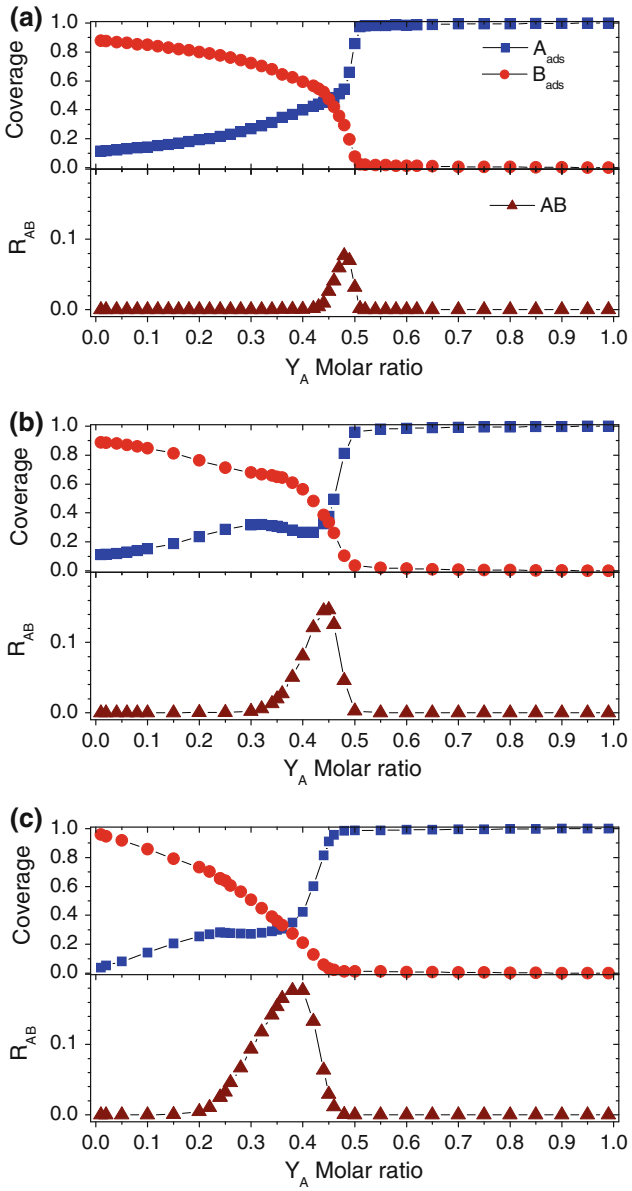

Fig. 3 Effect of particle deformation at 500 K in the case where no interactions are considered: **a** no diffusion considered, **b** CO diffusion considered, and **c** CO and M diffusion considered

metal surface with O atoms. In fact, the roughening of the metal particle leads now to configurations where the majority of metal terraces become poisoned with O, while the minority of terraces (especially those with just one metal atom) become poisoned with CO, therefore stopping the reaction. The inclusion of CO diffusion, as expected, expands the reaction window toward lower values of Y_{CO} and the reactivity is increased due to the fact that CO from a smaller terrace may reach the border of an O island on a larger terrace. The additional inclusion of M diffusion (c), meaning that the dynamic deformation of the metal particle continues during the reaction process, enhances even more the reaction window toward lower Y_{CO} values and the reactivity, because the mobility of metal atoms changing in a dynamic way the particle morphology depresses the geometric impediments for O_2 dissociative adsorption. At an even higher temperature, for example $T = 900$ K, the reaction window disappears in the cases where no diffusion and only CO diffusion are considered and only appears at low Y_{CO} values when both CO and M diffusion are taken into account (results not shown here). All these results are in good concordance with those already obtained in Ref. [14], although the curves in the present work are quite smoother due to a better statistics in the simulation procedure.

We proceed now to present the effects of lateral interactions for a given temperature, $T = 500$ K. In all cases the values considered for the interaction energy W_{AB} are: 0 (no interactions), +1 kJ/mol (repulsive interactions) and −1 kJ/mol (attractive interactions)[1]. Even though all possible combination of interactions and diffusion conditions were studied, we shall only present here some of the most relevant results.

Figure 4 shows the effects of CO–CO interactions when only CO diffusion is considered. Here we have the case of null interactions in part (a), repulsive interactions in part (b) and attractive interactions in part (c). As it can be easily understood, repulsive CO–CO interactions increase the reactivity while attractive interactions decrease the reactivity. Note that the reaction window is only modified in the case of repulsive interactions, shifting the right end toward higher values of Y_{CO}, this is so because repulsive interactions will difficult the formation of CO islands and therefore the poisoning of the surface with CO at high Y_{CO}. When instead O–O interactions are considered (figure not shown), attractive interactions practically do not modify the reaction window corresponding to the case of null interactions, due to the fact that even without attractive interactions compact

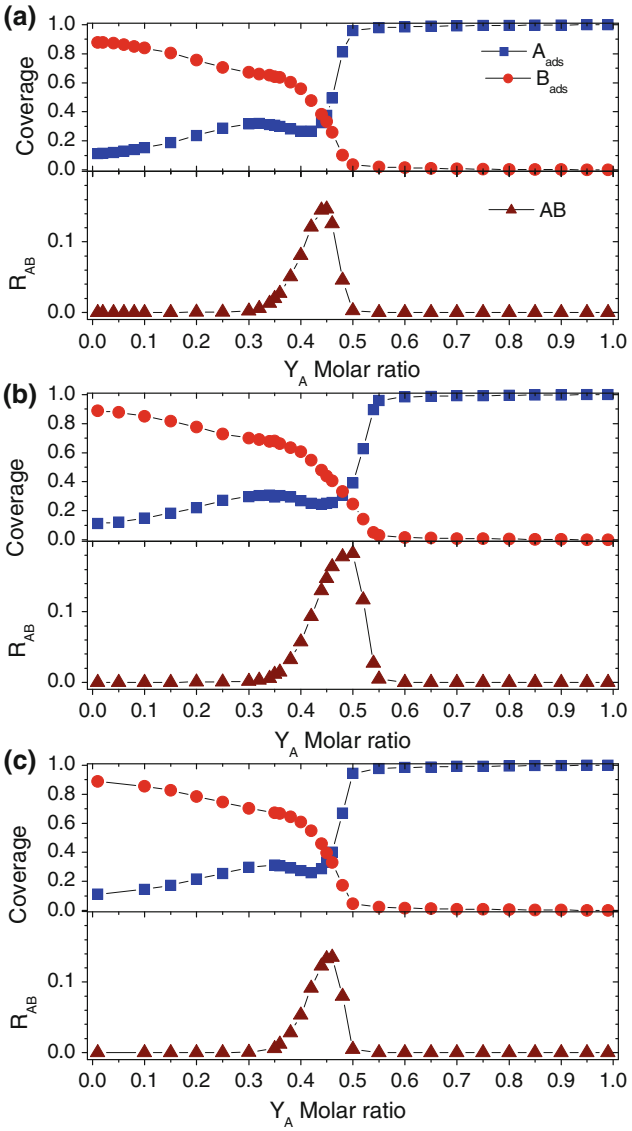

Fig. 4 Effect of CO–CO interactions at 500 K in the case where CO diffusion is considered: **a** null interactions, **b** repulsive interactions, and **d** attractive interactions

O islands are formed because of the O_2 adsorption mechanism, while repulsive interactions produce an important widening of the reaction window toward low Y_{CO} values because they will help to produce irregularly shaped vacant regions in those islands facilitating the reaction with CO species. When instead O–M interactions are considered (figure not shown), attractive interactions do not practically affect the reaction window, while repulsive interactions produce an even stronger effect that the one due to O–O repulsive interactions. In fact, the effect of O–M repulsive interactions in our model is that of making the sticking coefficient for O_2 adsorption less than 1 (and therefore less that that corresponding to CO), which is in better concordance with experimental observations as compared with the

[1] Other values for the intensity of lateral interactions were tested with similar results. The values of+ and − 1 kJ/mol are representative of small interactions, but sufficiently strong as to produce observable effects.

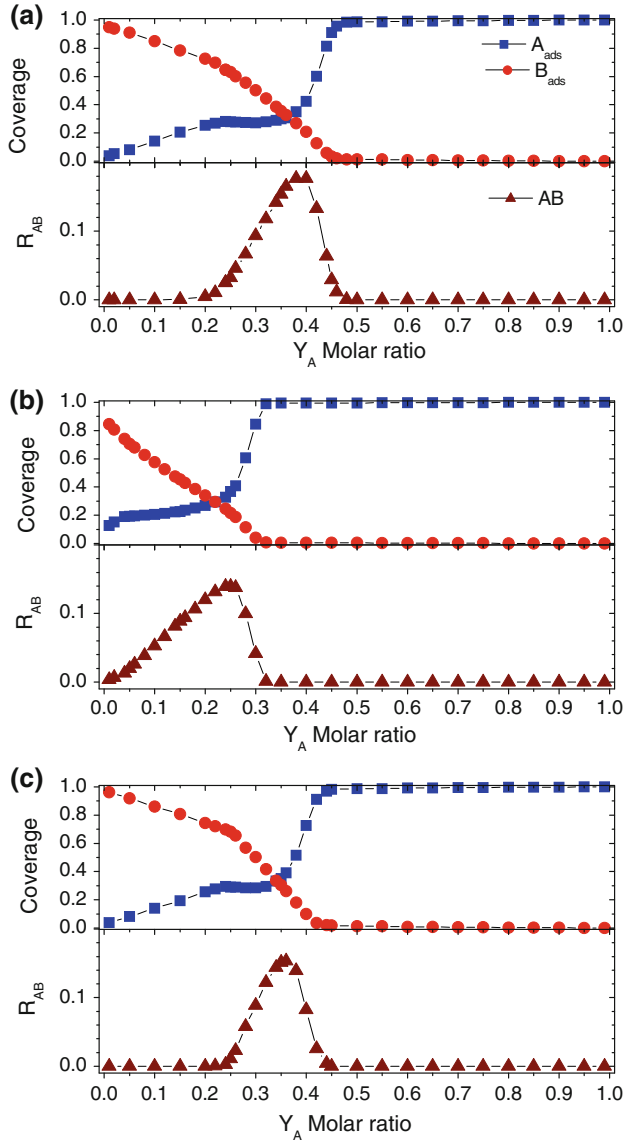

Fig. 5 Effect of O–M interactions at 500 K in the case where CO and M diffusion are considered: **a** null interactions, **b** repulsive interactions, and **d** attractive interactions

assumptions of the ZGB model (where both sticking coefficients are taken to be 1), and this is a more efficient mechanism in extending the reaction window to lower Y_{CO} values than O–O repulsive interactions. CO–O and CO–M interactions (results not shown here) do not produce any interesting effects besides the expected decrease in reactivity for repulsive interactions.

We discuss now the results corresponding to the more realistic case where both CO and M diffusion are taken into account. The behavior is similar to that described for the case just discussed where only CO diffusion is considered, with the difference that the reactivity and reaction windows are even more enhanced by the additional dynamic restructuring of the metal particle during the reaction, as explained above when commenting Fig. 3. However, it is very interesting to note that the behavior of the reactivity shown in Fig. 5b corresponding to O–M repulsive interactions, where the reaction window extends in a linear shape practically down to $Y_{CO} = 0$, is in very good concordance with the behavior observed experimentally by Ehasi et al. [15] for the CO oxidation reaction on a stepped Pt(210) surface at 500 K.

Table 1 Values of the reaction window opening (RWO) and the reaction window closing (RWC), in terms of Y_{CO}, and the maximum reaction rate (MRR) achieved, for the different cases presented in this study

Case	RWO	RWC	MRR
ZGB Model, undeformed particle	0.45	0.51	0.23
Undeformed particle + CO diffusion	0.12	0.51	0.38
Deformed particle at 500 K, no interactions			
No diffusion	0.42	0.51	0.08
CO diffusion	0.3	0.5	0.16
CO and M diffusion	0.18	0.49	0.18
Deformed particle at 500 K + CO diffusion			
Repulsive CO–CO interactions	0.35	0.68	0.19
Attractive CO–CO interactions	0.34	0.51	0.14
Repulsive O–O interactions	0.18	0.5	0.2
Attractive O–O interactions	0.3	0.5	0.16
Repulsive O–M interactions	0.12	0.4	0.14
Attractive O–M interactions	0.3	0.5	0.14
Deformed particle at 500 K + CO and M diffusion			
Repulsive CO–CO interactions	0.19	0.55	0.2
Attractive CO–CO interactions	0.2	0.5	0.17
Repulsive O–O interactions	0.1	0.45	0.21
Attractive O–O interactions	0.18	0.48	0.18
Repulsive O–M interactions	0.01	0.32	0.14
Attractive O–M interactions	0.24	0.45	0.18

The behavior of the reaction window for all cases considered is resumed in Table 1, where the values, in terms of Y_{CO}, of the reaction window opening (RWO), the reaction window closing (RWC) and the maximum reaction rate (MRR) achieved are given.

4 Conclusions

We have studied the CO oxidation reactions on supported metallic nanoparticles taking into account the particle deformation due to thermal effects, which produce metal atom diffusion, the diffusion of CO and adsorbate–adsorbate and adsorbate–metal interactions. The behavior of the reaction window and the reactivity in the steady state regime has been found to be affected by the thermal deformation, by CO and M diffusion and by some of the

interactions tested in this study, particularly CO–CO, O–O and O–M interactions. Such behavior, in each case, has been discussed and rationalized in such a way as to obtain an understanding of the process at a molecular level.

As the main result, it has been found that in the more realistic conditions, where CO and M diffusion and O–M repulsive interactions (meaning a sticking coefficient for O_2 less than 1) were considered, the predictions of the model are in very good concordance with experimental results obtained for the CO oxidation reaction on a stepped Pt(210) surface at 500 K [15].

The present study may contribute to the still far away objective of filling the gap between ideal and real catalytic systems.

Acknowledgements CONICET and FONCYT of Argentina are gratefully acknowledged for financial support to this research.

References

1. Somorjai GA, Li Y (2010) Top Catal. doi:10.1007/s11244-010-9449-0
2. Somorjai GA, Park JY (2008) Chem Soc Rev 37:2155
3. Henry CR (1998) Surf Sci Rep 31:231
4. Gunter PLJ, Niemantsverdriet JW, Ribeiro FH, Somorjai GA (1997) Catal Rev Sci Eng 39:77
5. Ramírez-Cuesta AJ, Bennet RA, Stone P, Mitchell PCH, Bowker M (2001) J Mol Catal A Chem 167:171
6. Bustos V, Uñac RO, Zgrablich G, Henry CR (2003) PCCP 5:2906
7. Kovalyov EV, Elokhin V, Myshlyavtsev AV (2007) J Comp Chem 29:79; and references therein
8. Kovalyov EV, Elokhin VI (2009) Chem Eng J 154:88
9. Avalos LA, Bustos V, Uñac R, Zaera F, Zgrablich G (2006) J Phys Chem B 110:24964
10. Uñac RO, Bustos V, Wilson J, Zaera F, Zgrablich G (2006) J Chem Phys 125:074705
11. Zaera F, Sales JL, Gargiulo MV, Ciacera M, Zgrablich G (2007) J Phys Chem C 111:7795
12. Ziff RM, Gulari E, Barshad Y (1986) Phys Rev Lett 56:2553
13. Wintherlin J, Völkening S, Janssens TVW, Zambelli T, Ertl G (1997) Science 278:1931
14. Kovalyov EV, Resnyanskii ED, Elokhin VI, Bal'zhinimaev BS, Myshlyavtsev AV (2003) Phys Chem Chem Phys 5:784
15. Ehasi M, Matloch M, Frank O, Block JH, Christmann K, Rys FS, Hirschwald W (1989) J Chem Phys 91:4949